SAND2015-1345C

V-Notched Rail Test for Shear-Dominated Deformation of Ti-6Al-4V

Sharlotte Kramer, John Laing, Thomas Bosiljevec, Jhana Gearhart, and Brad Boyce
Sandia National Laboratories, 1515 Eubank SE, Albuquerque, NM 87123, USA

Abstract

Evermore sophisticated ductile plasticity and failure models demand experimental material characterization of shear behavior; yet, the mechanics community lacks a widely accepted, standard test method for shear-dominated deformation and failure of ductile metals. We investigated the use of the V-notched rail test, borrowed from the ASTM D7078 standard for shear testing of composites, for shear testing of Ti-6Al-4V titanium alloy sheet material, considering sheet rolling direction and quasi-static and transient load rates. In this paper, we discuss practical aspects of testing, modifications to the specimen geometry, and the experimental shear behavior of Ti-6Al-4V. Specimen installation, machine compliance, specimen-grip slip during testing, and specimen V-notched geometry all influenced the measured specimen behavior such that repeatable shear-dominated behavior was initially difficult to obtain. We will discuss the careful experimental procedure and set of measurements necessary to extract meaningful shear information for Ti-6Al-4V. We also evaluate the merits and deficiencies, including practicality of testing for engineering applications and quality of results, of the V-notched rail test for characterization of ductile shear behavior.

Keywords: shear, failure, metals, mechanical properties, model calibration

Introduction

Several ductile plasticity and failure models such as the shear-modified Gurson model [1,2] require shear testing for calibration. The mechanics community has the ubiquitous uniaxial tensile test and compact tension fracture test for experimental characterization of tensile deformation and failure, but lacks a widely accepted method for shear-dominated behavior. Proposed experimental methods for this purpose include the Iosopescu geometry (ASTM D5379) [3,4], the punch geometry (ASTM D732), the Butterfly geometry [5], the Arcan shear [6], tension-torsion fracture [7], and the V-notched rail shear (ASTM D7078) [8,9]. These methods vary in complexity of setup, specimen design, measurements, boundary conditions, and data interpretation, all leading to a difficult choice of method depending on the material of interest, cost and time considerations, and the available experimental lab facilities.

The motivation for the shear testing in this paper was the second Sandia Fracture Challenge (SFC), which was a blind round robin prediction of ductile tearing by the computational mechanics community. Sandia National Laboratories hosted the first SFC in 2012, where computationalists were charged to predict ductile failure in a "crack-in-a-maze" geometry in 15-5PH stainless steel, based on standard material characterization experimental data from uniaxial tension and compact tension fracture tests [10]. The assessment of the first SFC showed that no computational team could properly predict all the features of the failure; one area of improvement for the predictions noted by the challenge participants was providing shear-dominated material characterization data. The second SFC, in 2014, was another "crack-in-a-maze" geometry, but in Ti-6Al-4V at two loading rates, one quasi-static and one at a modest transient rate, and the material characterization experimental data was from uniaxial tension tests and shear-dominated tests, as requested by the first SFC participants.

In this present paper, we discuss the use of the V-notched rail shear test to investigate the shear behavior of Ti-6Al-4V for quasi-static and transient loading rates for the second SFC. The V-notched rail shear test was first developed for composite materials, but we demonstrate that this method can be used for metals, provided careful procedures are followed. Local strain and displacement measurements, fixture compliance tests, careful gripping procedures, characterization of specimen slip in the grips, and specimen design are all factors for successful, repeatable tests, but interpretation of the data through the large deformations and failure regimes requires computational modeling to extract meaningful material characterization data.

Experimental Setup and Testing Procedure

Fixture and Measurements

The V-notched rail test requires special grips, as prescribed by ASTM D7078; we obtained the adjustable combined loading shear (CLS) fixture from Wyoming Test Fixtures as shown in Fig. 1. The CLS fixture has approximately 50.8 mm x 50.8 mm of gripping area on each half of the fixture, adjusts to different specimen thicknesses, and provides a 25.4-mm central gap between the grip halves where the double V-notch feature of the specimens undergoes shear-dominated deformation. The 17-4 PH stainless steel fixture has sixteen 5/8-18 UNC stainless bolts (two tall, two wide on each face) to secure the specimens. To measure the local displacement of the two fixture halves relative to each other, we installed an axial linear variable differential transformer (LVDT) (Measurement Specialties MHR open core LVDT, +/- 12.7-mm range) across the vertical gap of the fixture halves in line with the actuator, as shown in Fig. 1. To measure relative rotation of the fixture about the z-axis (specimen thickness), we attached two lateral LVDTs (Macro Sensors BBP 315-100 LVDT, +/- 0.254-mm range) to the front face of the fixture, above and below the gripping bolts, perpendicular to the actuator. The fixture was installed in a 100-kN MTS, two-post, servo-hydraulic, single actuator load frame with a 100-kN MTS load cell.

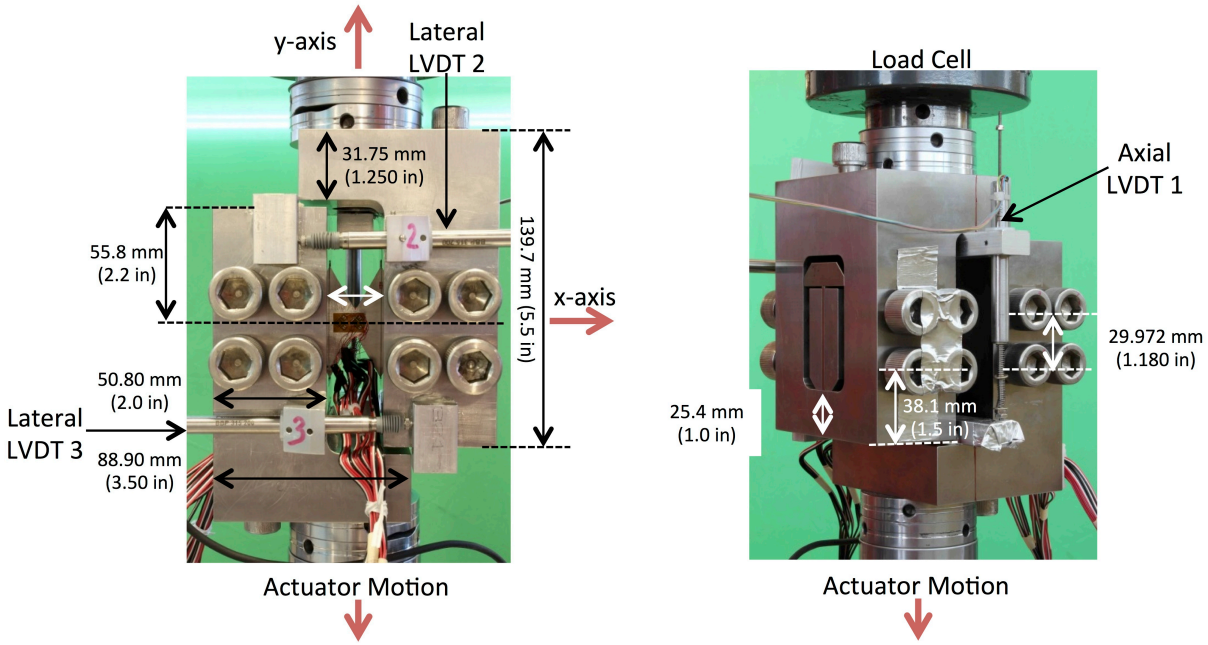

Figure 1 - Wyoming Test Fixtures Adjustable Combined Loading Shear Fixture, as installed in a 100-kN MTS two-post, servo-hydraulic, single-actuator load frame, with a strain-gaged double V-notched specimen: (left) front view of the fixture with attached lateral LVDTs and reference blocks; (right) rear view of the fixture with attached axial LVDT and reference block.

Preliminary Testing and Test Procedure Modifications

When this fixture is used for composite materials, strains measured by strain gages, applied to the center of the specimen, and the load history are sufficient to characterize the shear stress-strain behavior. In the case of a ductile metal specimen, the strains are often larger than the range of conventional strain gages, requiring a computionalist to model the test to extract shear properties of the metal. Without local displacement / strain measurement on the surface of the specimens, the computationalist having only have global fixture measurements would need to compensate for fixture compliance and any other specimen behavior. Therefore, we needed to perform compliance testing and measure fixture motion during the tests. Prior to compliance testing, we performed preliminary tests to determine the load range and fixture behavior on a few specimens to develop an appropriate testing approach.

Preliminary testing of specimens with the standard 90-degree V-notches from the 3.124-mm thick Ti-6Al-4V plate material had several issues that had to resolved to get reasonable data. The large loads required to fail the specimens led to significant

rotations about the z-axis of the fixture halves (through-thickness axis) as measured by the lateral LVDTs (on the order of 0.5 mm relative displacement), causing significant slip of the specimens in the grips and considerable galling of the specimen gripping surfaces. The large torque on the gripping bolts required to secure the specimen, approximately 67.8 N-m (50 ft-lbs), would sometimes cause the bottom half of the fixture to rotate with the actuator, bending the specimen about the actuator axis (y-axis). Alignment of the fixture halves and the specimen during gripping was challenging to maintain. These issues are presumably not present for composite materials, which would require much lower loads for failure and lower torque on the bolts for specimen installation.

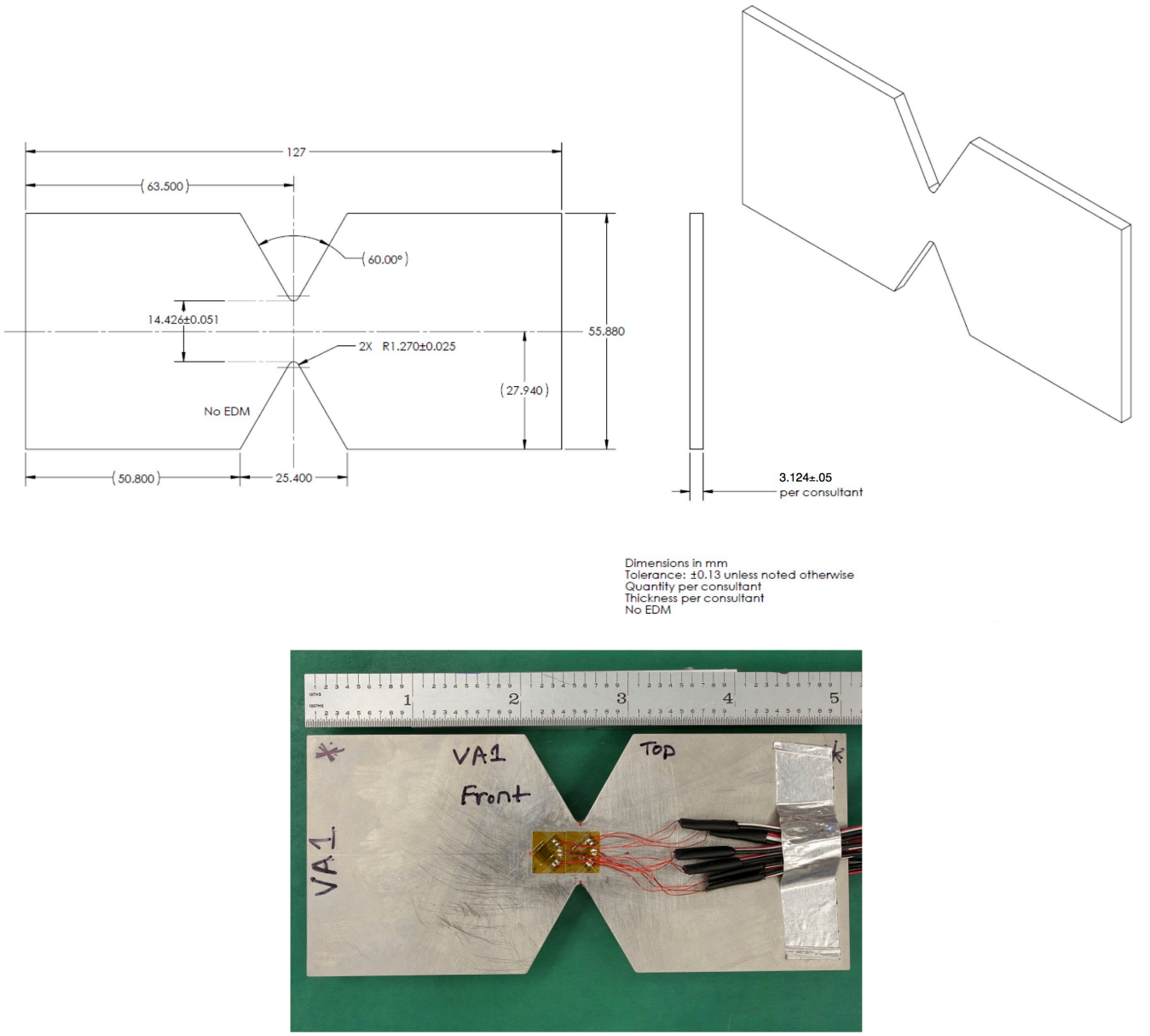

Figure 2 - Modified specimen geometry for the 3.124-mm thick Ti-6Al-4V plate with 60-degree deep V-notches: (top) specimen fabrication drawing; (bottom) specimen VA1 with attached strain gage rosettes in the center of the gage section, shown with a ruler in inches.

Modification of the specimen geometry and development of careful specimen installation procedures resolved these issues with the setup. With the 25.4-mm V-notch width set by the 25.4-mm gap in the test fixture, we cut deeper V-notches at 60-degrees into the specimens instead of the standard 90-degree, as shown in Fig. 2, in order to reduce the area between the notches, thus reducing the maximum load of the test. The lower maximum load in turn significantly reduced the fixture rotation about the z-axis; all tests with these modified tests led to negligible relative displacements of the lateral LVDTs. The

specimen installation procedure utilized stacked rosette strain gages from Micro-Measurements (Model CA2-06-125WW-350), with gage length 3.18 mm (0.125 inch) and 3% strain measurement range, attached to the front and back of each specimen. The strain gages were located in the center of the specimen and to the side of center closer to the left (bottom) fixture half. The installation procedure required that the strain not rise more than 100-microstrain on any gage as the gripping bolts were tightened, providing confidence that the specimen was not bent or twisted during installation. Also, the bolts on the left (bottom) fixture half were gradually tightened, such that the eight bolts were all tightened in 13.6 N-m (10 ft-lbs), increments up to 67.8 N-m (50 ft-lbs), as opposed to each bolt individually torqued to 67.8 N-m (50 ft-lbs). The specimen underwent precycling of the actuator to loads of +/- 4.448 kN in order to assess how the strain gages and specimen are behaving in the elastic regime. If the strain gages on the two faces of the specimen indicated unwanted bending in the specimen, then the specimen was removed and then reinstalled. These changes to the experimental procedure and specimen allowed for reasonable test data, but the specimens did continue to slip slightly throughout the test. We characterized this specimen slip behavior so that the slip could be accounted for in the data, as will be described.

Eight V-notched Ti-6Al-4V specimens were tested: four each with the dominant shear loading direction aligned with the rolling direction (denoted VA) and perpendicular to the rolling direction (denoted VP). Specimens VA1, VA2, VP2, and VP6 were tested at an actuator rate of 0.0254 mm/s, and specimens VA3, VA4, VP3, and VP4 were tested at 25.4 mm/s. The testing protocol included strain gage installation on each specimen, the above specimen installation in the fixture, the precycles of +/- 4.448 kN, and then the monotonic pull to failure at the prescribed actuator displacement rate.

Compliance and Specimen Slip Characterization

The lateral stiffness of each fixture half was characterized. A 2.224-kN (0.50-kip) load cell was attached to a manual pull rod and a clevis. The clevis was attached to a rod end bearing gripped in one half of the fixture, as shown in Fig. 3. The manual pull rod allowed the operator to apply a lateral load to each half of the fixture to measure the lateral displacements of fixture. As seen in Fig. 3, the lateral stiffness of the upper fixture half (attached to the stationary part of the load frame) is greater than the lower fixture half (attached to the actuator). The upper fixture half has more rotation for a given load than the lower fixture half as seen in the difference between lateral LVDTs. This data shows how much lateral load is required to displace the fixture halves laterally; in turn, the lateral displacement measured during the V-notched specimen tests can be related to the lateral stiffness measured here. The V-notched specimen tests had negligible lateral displacements, implying that the specimens did not exhort significant lateral loads on the fixture.

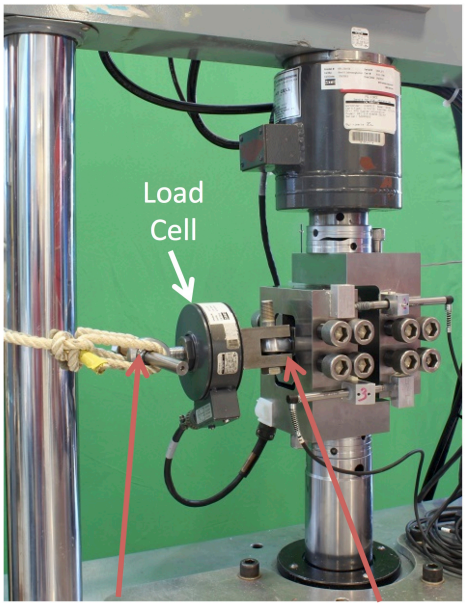

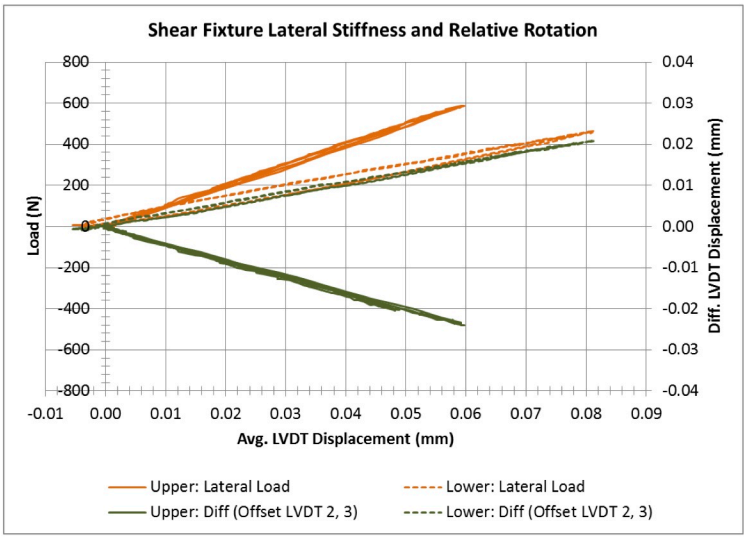

Figure 3 - Fixture Lateral Compliance Test: (left) test setup; (right) load and relative displacement difference between the lateral LVDTs versus the average lateral LVDT displacement.

The fixture had significant axial compliance that required characterization so that computationalists could utilize the load-axial displacement data for material characterization. The fixture compliance characterization tests were completed using two different plates: a generic alloy steel with dimensions 55.766-mm x 129.29-mm x 9.385-mm (2.1955-in x 5.090-in x 0.36975-in) and the Ti-6Al-4V with dimensions 55.88-mm x 127.36-mm x 3.061-mm (2.200-in x 5.014-in x 0.1205-in). Each plate had four sets of three strain gages similarly located as on the V-notched specimens. The plates were installed in the same manner as described for the V-notched specimens and then were subjected to a set of cyclic loading to various load levels at 0.1-Hz rate, to a maximum of 35.6 kN, which is larger than the maximum load of the V-notched Ti-6Al-4V specimens. Then the plates then underwent the same set of cyclic loads without removal of the plates. The load versus axial LVDT displacement data is given in Fig. 4. The axial compliance tests revealed two main effects: nonlinear compliance of the test fixture and specimen slip in the grips. It is possible that these two factors can be taken into account by applying a first-order linear correction to load vs. axial LVDT data so that the modulus matches the strain-gage data. We have also made an attempt to characterize these factors independently through the compliance tests, offering another more detailed possibility to account for specimen slip and fixture compliance through computational modeling of the experiment.

With regards to specimen slip, for the first set of cyclic loads in each plate, the amount of displacement for the first monotonic loading from zero to the upper bound of each load level is larger than each subsequent cycle segment for that load level; also the remaining cycle segments return to the same displacement. This implies that the specimen slip predominately occurred upon the initial positive loading through a load regime; in other words, the cyclic loading exhibits considerable slip on the first portion of increasing load with little accumulation of additional slip in subsequent cycles between the same two load end-points. When the Ti-6Al-4V plate underwent the a second set of cyclic loading without the plate being removed, the plate did not accumulate any more slip, as shown in Fig. 4 bottom right, so the behavior here is just due to fixture compliance. The slip behavior of the steel plate was less pronounced than that of the Ti-6Al-4V plate because the steel plate grip surfaces were visibly rough as compared to those of the smooth Ti-6Al-4V plate. The slip behavior of the Ti-6Al-4V compliance test plate is assumed to be the same as that of the V-notched specimens; thus, these Ti-6Al-4V plate compliance tests allow for empirical characterization of the slip behavior.

This empirical characterization can be applied to the V-notched specimen tests to remove the effect of slip in the axial LVDT data, assuming the same slip behavior is present for the two loading rates of the V-notched specimen tests. As previously mentioned, the V-notched specimens underwent precycles of +/- 4.448 kN to assess the strain gage and specimen behavior after installation prior to the monotonic pull to failure; the axial LVDT was zeroed after the precycles, so slip accumulated between 0 and 4.448 kN was assumed to be removed from the monotonic pull data. Therefore, to remove the accumulated slip from the axial LVDT data for the monotonic pull to failure portion of the V-notched specimen data, an empirical formula based on the slip seen in the Ti-6Al-4V plate compliance test was applied to the V-notched monotonic pull data *above* the 4.448-kN (1000-lbs) precycle level. The empirical formula for slip in the increasing load portion of the Ti-6Al-4V plate compliance test was derived in the following manner. The slip accumulated on the initial monotonic pull between two load levels (the maximum load of the prior precycle and the new maximum load of the current precycle), as seen by the axial LVDT, was assumed to be the difference in the axial LVDT values at zero load for the first complete cycle of the current precycle set. This was taken at zero load because there is no fixture compliance at zero load, and thus the difference in the axial LVDT measurement after one cycle was assumed to be due to specimen slip on the increasing load segment. For example, to calculate the slip between 4.448 kN and 8.896 kN, one would subtract the axial LVDT values at the end and start of the first cycle of the 0 to 8.896-kN precycle set. In other words, one assumes the slip between 0 and 4.448 kN has already occurred in the prior 0 and 4.448-kN precycle set, so comparing the end values of the Axial LVDT 1 of the first cycle of the 0 to 8.896-N precycle set should provide the slip between 4.448 kN and 8.896 kN. This exercise was repeated for each precycle set in increments of 4.448 kN (1000 lbs) up to 35.586 kN (8000 lbs), and then a power-law curve was fit to the accumulated-slip-in-Axial-LVDT-1 vs. Load-above-the-precycle-set curve, shown in Fig. 5, for two separate Ti-6Al-4V plate compliance tests. [Note: The small amount of slip accumulated in subsequent cyclic loadings is ignored in this empirical relationship because the V-notched specimen tests have only a monotonic axial displacement, and thus extra slip in the compliance tests would not be present in the V-notched specimen tests. There is also an implicit assumption that no slip occurs for decreasing load in the monotonic pull segment in the V-notched specimen tests.] Since the first compliance test had unblemished surfaces, we used the curve fit from the first compliance test for slip removal:

$$(Slip) = 8.528 * 10^{-4} * (Load - 4.448)^{1.435}\ mm \quad (1)$$

Once maximum load is reached, it is assumed that the slip does not decrease with the load drop, so the maximum slip value is subtracted from axial LVDT reading for decreasing loads after maximum loads. For example, in specimen VA2 shown in Fig. 5, the maximum load was 29.658 kN with an associated slip of 0.0876 mm, and that amount of slip was removed from the axial LVDT for all displacements after maximum load had been achieved.

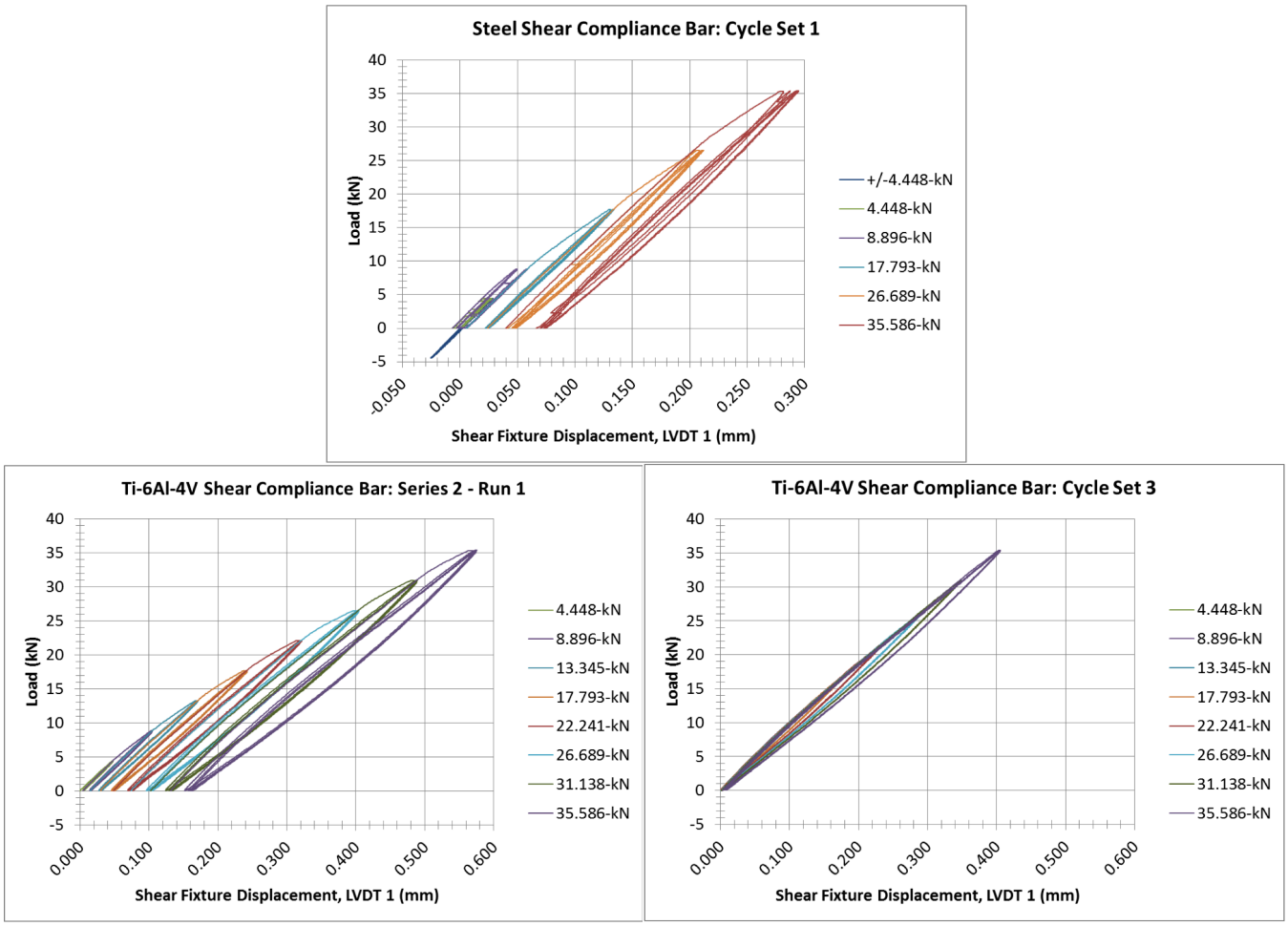

Figure 4 - Compliance behavior of the CLS fixture with Steel and Ti-6Al-4V plates: (Top) compliance behavior with a steel plate, including plate grip slip; (bottom left) compliance behavior with a Ti-6Al-4V plate for the first set of cyclic loads, with plate grip slip; (bottom right) compliance behavior with a Ti-6Al-4V plate for the third set of cyclic loads, without significant plate grip slip.

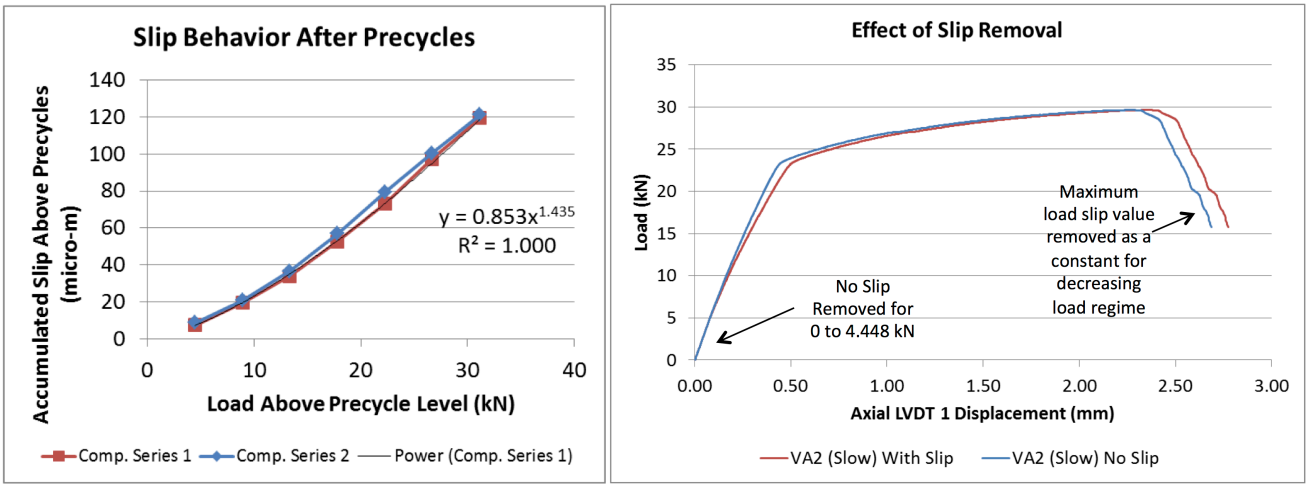

Figure 5 - Slip in the Ti-6Al-4V Specimens: (left) empirical fit to characterize specimen slip; (right) load vs. axial LDVT displacement with and without slip removed.

The compliance behavior of the fixture, uncorrupted by specimen slip, is apparent last cycle between 0 and 35.6 kN and in the cycle sets after the first cycle set (see Fig. 4), as previously mentioned. The behavior in these cyclic loads included both the elastic deformation of the plates and fixture compliance. An estimate of these relative magnitudes of the fixture compliance and elastic deformation of the compliance plate is as follows. The fixture displacement is approximately 0.30 mm at 26.7 kN for the Ti-6Al-4V plate. Using a simple calculation for simple shear in the elastic regime for the Ti-6Al-4V with a 44-GPa shear modulus, the relative vertical displacement, measured by the axial LVDT, of the 55.88-mm x 25.4-mm x 3.061-mm (2.200-in x 1.0-in x 0.1205-in) section in the grips, would be approximately 0.09 mm at 26.7 kN. This implies that the fixture compliance is about 0.21 mm at 26.7 kN, which is on the order of 10-20% of the fixture displacement at maximum load of the VP V-notched specimens. A computationalist would be advised to account for this fixture compliance when modeling this experiment because the compliance is not negligible.

Results and Discussion

For all eight specimens, the calculated shear stress versus shear strain data for the portion of the test where the central strain gages were attached to the specimens are provided in Fig. 6. The elastic modulus from the shear stress-strain data is 44 GPa, which is consistent with literature values [11]; thus, this experimental approach does appropriately apply a shear-dominated deformation in the center of the specimens, allowing for characterization of shear-dominated behavior of Ti-6Al-4V using strain gages in the low-strain regime. The shear stress-strain data shows that Ti-6Al-4V is rate-sensitive, with higher a yield stress at an actuator rate of 25.4 mm/s versus that at quasi-static rates. The low-strain regime for the two rolling directions does not show significant anisotropic yield behavior in shear at both displacement rates.

The data from the strain gages gives confidence that the experimental technique is reasonable for metals, but is not sufficient to characterize the large shear deformation and failure behavior; the load-displacement data, despite the issues with specimen slip and fixture compliance, do provide the potential for this characterization in conjunction with computational modeling. The load-displacement data, still including the specimen slip and fixture compliance, are given in Fig. 7, showing anisotropic plastic behavior between the two rolling directions and strain-rate dependence of the plastic behavior, with different maximum loads, displacement at maximum load, and displacement to failure. For both rolling directions, the faster rate specimens reached maximum load earlier and failed earlier than the quasi-static rate specimens.

Fig. 8 is a compilation of failed specimens viewed from the front of the specimen and along the through-thickness of the fracture surfaces. In all of the specimens, the crack did not propagate from the roots of the V-notches, but rather at the side of the roots at an angle to the opposite side. The crack paths of the VA specimens, with their rolling direction aligned with the shear directions, were rather jagged at the quasi-static loading rates; the other crack paths were straighter. We observed negligible lateral displacement of the fixture during the VA quasi-static tests, so this not due to rotation of the grips , but rather to some phenomenon that requires further investigation. The width of the shear-dominated deformation region in the center of the specimens was larger for the quasi-static rates for both rolling directions.

There are a few areas of improvement for this technique for shear-dominated loading. First, one potential method for extracting the calculated shear stress-stain behavior for the entire deformation is Digital Image Correlation (DIC). The relatively large visible area of interest of the V-notched specimens in this fixture would make DIC a straightforward method for local displacement / strain measurements, providing flexibility in selection of the virtual strain gage length and location. Second, the gripping mechanism could be greatly improved beyond the current bolt-fastened grips. Hydraulic gripping with a constant pressure would provide an even gripping pressure over the entire gripping area; the hydraulic pressure could be set to a greater value than that achievable with the bolt-fastening approach. Also, the grip faces could be surface-treated to have a rougher gripping surface to reduce slip. An improved gripping mechanism would increase testing throughput and enhance repeatability. Third, the specimen could be modified to have (1) a thinner thickness as to lower the overall load required, but this may lead to issues with specimen bending during installation, (2) other angles for the V-notches to alter the load required, and (3) a roughened grip surface to reduce specimen slip.

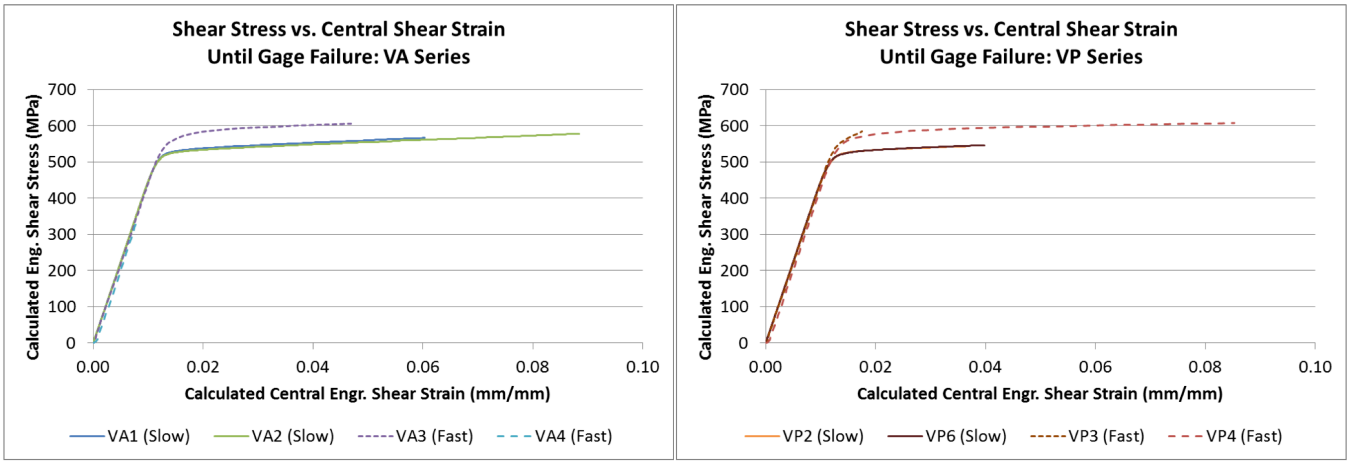

Figure 6 - Calculated Shear Stress vs. Shear Strain for the V-notched Ti-6Al-4V Specimens: (left) VA series specimens; (right) VP series specimens [Note: the end of each line indicates when the strain gages delaminated from the specimen.]

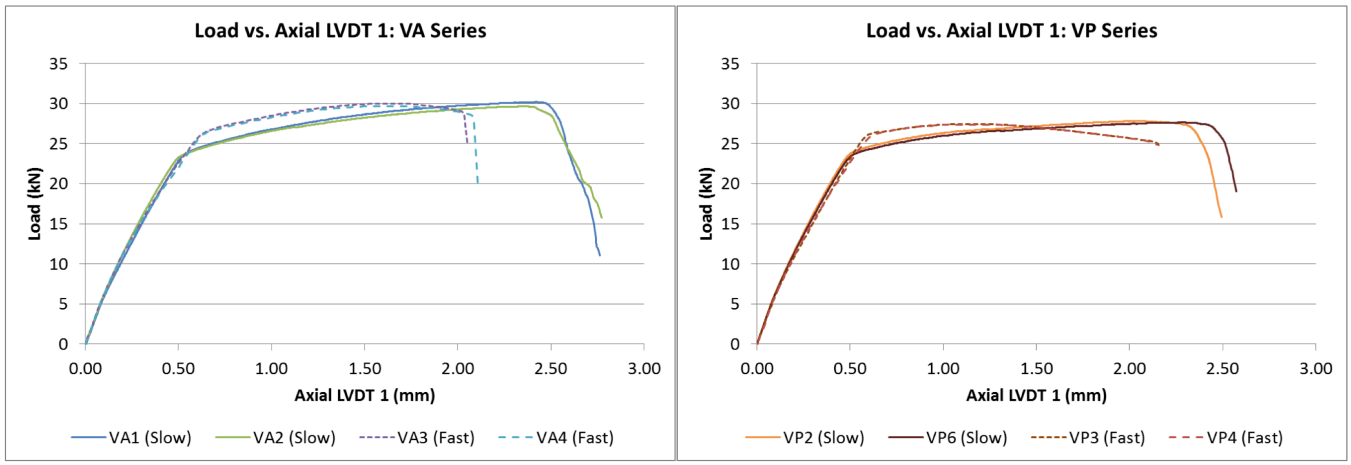

Figure 7 – Load vs. Axial LVDT Displacement for the V-notched Ti-6Al-4V Specimens: (left) VA series specimens; (right) VP series specimens [Note: this data includes the fixture compliance and specimen slip, hence the elastic regime is not linear like the shear stress vs. shear strain data.]

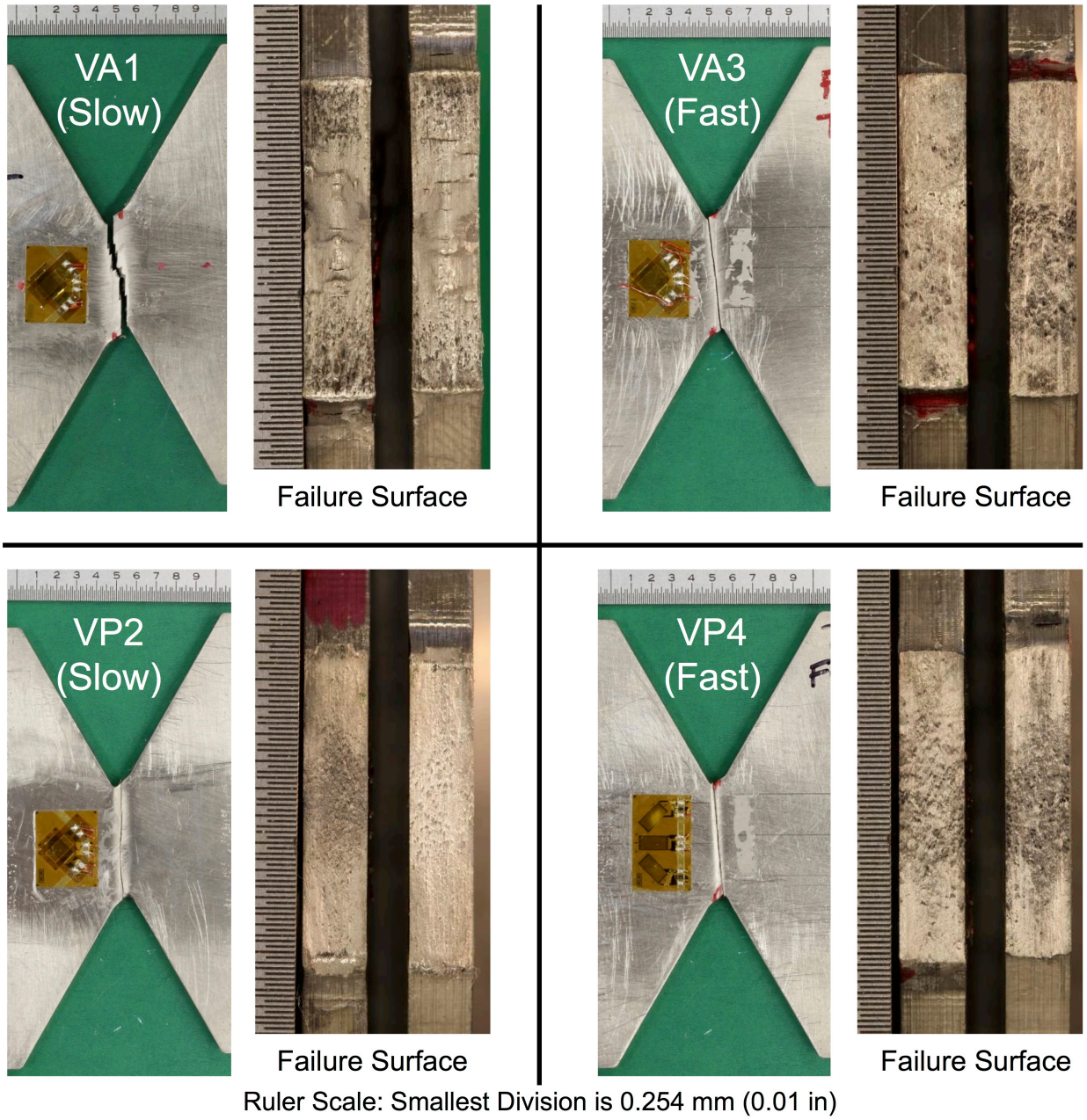

Figure 8 - Post-test images of four V-notched specimens, including the front face views and the failure surfaces.

Conclusion

We evaluated the use of the V-notched rail test for characterization of shear-dominated deformation and failure of Ti-6Al-4V. Using a modified V-notched specimen and careful procedures for specimen installation, we determined that the shear stress-strain data from strain gages gave credible elastic shear modulus measurements, providing confidence that the test was performing as expected, at least in the low-strain regime. Large fixture compliance and specimen slip obscured direct use of the load-displacement data for engineering calculations. Two approaches for compensation include (1) a first-order linear correction to the data such that the modulus from the corrected load-displacement data matches the strain-gage data, and (2) direct computational modeling of the experiment. The latter requires careful experimental characterization of the specimen slip and fixture compliance, which we completed through cyclic loading of stiff solid plates made of Ti-6Al-4V and alloy steel over the range of loads for the V-notched specimen tests. Modifications to the gripping mechanism and to the test specimen would help to reduce the specimen slip and reduce the testing loads in future tests. DIC could greatly increase the efficacy of the V-notched rail test: strain measurements over the gage section for the entire test could eliminate the need for

fixture compliance compensation since we would have the shear stress-strain relationship for the entire test from the measured load, DIC data and test geometry. With these improvements, the V-notched rail test appears promising as a test methodology for characterization of shear-dominated deformation and failure of ductile metals. As is, the V-notched rail test requires considerable computational effort to interpret the test results at large deformations.

Acknowledgements

Sandia is a multiprogram laboratory operated by Sandia Corporation, a Lockheed Martin Company, for the United States Department of Energy under contract DE-AC04-94AL85000.

References

[1] Nahshon, K. and Hutchinson, J.W. "Modification of the Gurson Model for shear failure." European Journal of Mechanics A-Solids 27 (1): 1-17, 2008.

[2] Xue, Z., Pontin, M.G., Zok, F.W., and Hutchinson, J.W. "Calibration procedures for a computational model of ductile fracture." Engineering Fracture Mechanics 77 (3): 492-509, 2010.

[3] Iosipescu, N. "New accurate procedure for single shear testing of metals." Journal of Materials 2 (3): 537-&, 1967.

[4] Adams, D.F. and Walrath, D.E. "Further development of the Iosipescu shear test method." Engineering fracture mechanics 27 (2): 113-119, 1987.

[5] Dunand, M. and Mohr, D. "Optimized butterfly specimen for the fracture testing of sheet materials under combined normal and shear loading." Engineering Fracture Mechanics 78 (17): 2919-2934, 2011.

[6] Ghahremaninezhad, A. and Ravi-Chandar, K. "Ductile failure behavior of polycrystalline Al 6061-T6 under shear dominant loading." International Journal of Fracture 180 (1): 23-28, 2013.

[7] Xue, Z., Faleskog, J., and Hutchinson, J.W. "Tension–torsion fracture experiments – Part II: Simulations with the extended Gurson model and a ductile fracture criterion based on plastic strain." International Journal of Solids and Structures 50 (25-26): 4258-4269, 2013.

[8] Adams, D.O., Moriarty, J. M., Gallegos, A.M., and Adams, D.F. "Development and Evaluation of thed Rail Shear Test for Composite Laminates." Federal Aviation Administration Report DOT/ FAA/AR-03/63, FAA Office of Aviation Research, Washington, D.C., September, 2003.

[9] Adams, D.O., Moriarty, J.M., Gallegos, A.M., and Adams, D.F., "The V-Notched Rail Shear Test." *Journal of Composite Materials*, 41 (3): 281–297, 2007.

[10] Boyce, B.L., *et.al.* "The Sandia Fracture Challenge: blind round robin predictions of ductile tearing." *International Journal of Fracture*, 186, (1-2): 5-68, 2014.

[11] Fukuhara, M. and Sanpei, A. "Elastic-moduli and internal frictions of Inconel 718 and Ti-6Al-4V as a function of temperature." *Journal of Materials Science Letters*, 12, (14): 1122-1124, 1993.